

SUPPORTING INFORMATION

On the importance of ferromagnetic exchange between transition metals in field-free SMMs: example of ring-shaped hetero-trimetallic $[(\text{LnNi}_2)\{\text{W}(\text{CN})_8\}]_2$ compounds

Sébastien Dhers,^{a,b} Jean-Pierre Costes,^{a,b} Philippe Guionneau,^c Carley Paulsen,^{d,e} Laure Vendier,^{a,b} Jean-Pascal Sutter^{*a,b}

^a CNRS; LCC (*Laboratoire de Chimie de Coordination*); 205, route de Narbonne, F-31077 Toulouse, France. E-mail: sutter@lcc-toulouse.fr

^b Université de Toulouse; UPS, INPT; LCC ; F-31077 Toulouse, France

^c CNRS, Université de Bordeaux, ICMCB, 87 Av. Doc. A. Schweitzer, 33608 Pessac, France

^d CNRS, Institut NEEL, F-38042 Grenoble, France

^e Université Grenoble Alpes, Institut NEEL, F-38000 Grenoble, France

EXPERIMENTAL:

Magnetic studies: Magnetic susceptibility measurements were carried out with a Quantum Design MPMS-5S SQUID magnetometer. The magnetic measurements were performed on freshly isolated polycrystalline materials. The samples were mixed with grease and put in gelatin capsules. DC measurements were conducted from 300 to 2 K at 1 kOe and the data were corrected for the diamagnetic contribution of the sample holder, grease and sample by using Pascal's tables.¹ The field dependences of the magnetization were measured at 2 K with dc magnetic field up to 5 T. AC susceptibility for **1a,b** and **2** was investigated under an oscillating ac field of 3 Oe over the frequency range of 1 to 1500 Hz. In addition, low temperature susceptibility and magnetization measurements up to 8 tesla were performed on sample **1a** using a high-field low-temperature SQUID magnetometer developed at the Institut Néel (Grenoble). The magnetometer is equipped with a miniature dilution refrigerator capable of cooling samples below 100mk and absolute values of susceptibility or magnetization can be made using the extraction method. As above, freshly isolated polycrystalline powder was mixed with Apiezon grease, then placed inside a copper pouch and attached to the copper sample holder of the dilution refrigerator. Measurements of the ac susceptibility were also made, extending the frequency range for this sample down to 0.021 Hz.

X-ray crystallographic studies: Single crystals suitable for X-ray diffraction of **1a-c** were collected at 150K on a κ-CCD Nonius diffractometer. All details are given in table S1. Note that samples of **1a** are actually made of poly-crystals leading to an overlap of Bragg intensities, probably responsible for the relatively average quality of the **1a** crystal structure in comparison to the satisfactory **1b,c** crystal-structure refinement final criterions. High level residual electronic density is found near the W atoms, notably in the **1a** crystal structure. This has been attributed to the relatively low quality of single crystals. All **1** compounds diffract only at low theta angle. Elsewhere, all H atoms were positioned on calculated position. Those of water molecules were positioned using the Nardelli method.² Structural determination, refinement calculations and handle of the data were made in the Wingx environment.³

Data for **2** were collected at low temperature (180 K) on an Xcalibur Oxford Diffraction diffractometer using a graphite-monochromated Mo-K α radiation ($\lambda = 0.71073\text{\AA}$) and equipped with an Oxford Instrument Cooler Device. The final unit cell parameters have been obtained by means of a least-squares refinement. The structures have been solved by Direct Methods using SIR92,⁴ and refined by means of least-squares procedures on a F2 with the aid of the program SHELXL97⁵ include in the softwares package WinGX version 1.63.⁶ The

¹ O. Kahn, *Molecular Magnetism*, VCH, Weinheim, 1993.

² M. Nardelli *J. Appl. Cryst.* 1999, **32**, 563

³ LJ Farrugia *J. Appl. Cryst.* 2012, **45**, 894-854

⁴ SIR92 - A program for crystal structure solution. A. Altomare, G. Cascarano, C. Giacovazzo and A. Guagliardi, *J. Appl. Crystallogr.* 1993, **26**, 343-350.

⁵ SHELX97 [Includes SHELXS97, SHELXL97, CIFTAB] - Programs for Crystal Structure Analysis (Release 97-2). G. M. Sheldrick, Institut für Anorganische Chemie der Universität, Tammanstrasse 4, D-3400 Göttingen, Germany, 1998.

⁶ WINGX - 1.63 Integrated System of Windows Programs for the Solution, Refinement and Analysis of Single Crystal X-Ray Diffraction Data. L.Farrugia, *J. Appl. Crystallogr.* 1999, **32**, 837-838.

Atomic Scattering Factors were taken from International tables for X-Ray Crystallography.⁷
All hydrogens atoms were geometrically placed and refined by using a riding model.

All non-hydrogens atoms were anisotropically refined, and in the last cycles of refinement a weighting scheme was used, where weights are calculated from the following formula:
 $w=1/[\sigma^2(Fo)^2+(aP)^2+bP]$ where $P=(Fo^2+2Fc^2)/3$.

It was not possible to resolve diffuse electron-density residuals (enclosed solvent molecule). Treatment with the SQUEEZE facility from PLATON⁸ resulted in a smooth refinement. Since a few low order reflections are missing from the data set, the electron count will be underestimated. Thus, the values given for D(calc), F(000) and the molecular weight are only valid for the ordered part of the structure. We are aware about the high residue closed to the Tb atom. Although we made semi-empirical absorption corrections, the residue is still there.

Drawing of molecule are performed with the program ORTEP32⁹ with 30% probability displacement ellipsoids for non-hydrogen atoms.

⁷ INTERNATIONAL tables for X-Ray crystallography, 1974, Vol IV, Kynoch press, Birmingham, England.

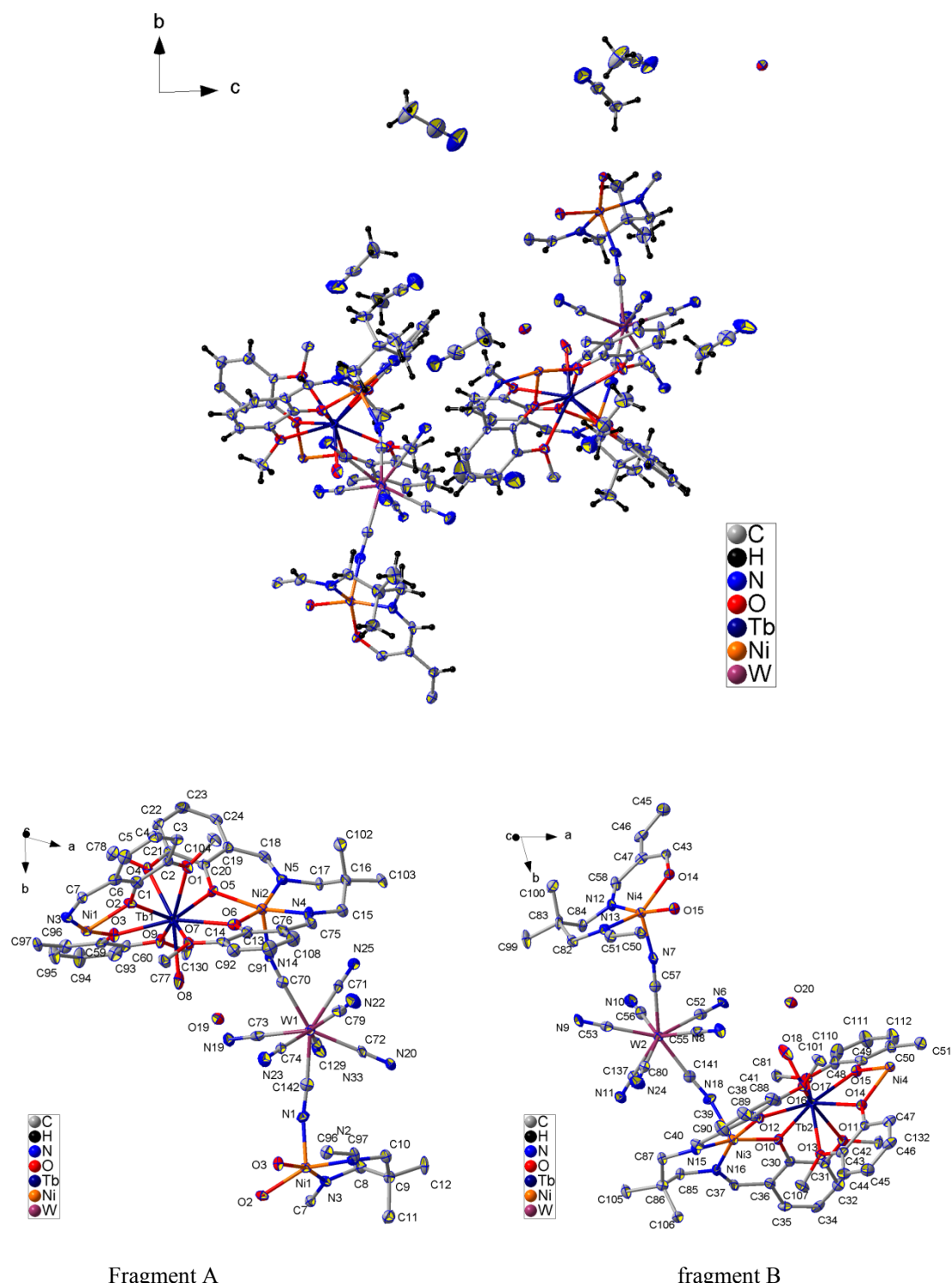
⁸ Sluis, P. v.d. and Spek, A. L. *Acta Cryst.* 1990, **A46**, 194-201.

⁹ L. J. Farrugia, *J. Appl. Crystallogr.* 1997, **30**, 565.

Table S1: crystallographic data and refinement parameters of the complexes **1a,b,c–2**

	1a	1b	1c	2
Formula moiety	[C ₁₀₀ H ₁₀₀ N ₂₄ O ₁₈ Ni ₄ Tb ₂ W ₂]. 10(CH ₃ CN).2H ₂ O	[C ₁₀₀ H ₁₀₀ N ₂₄ O ₁₈ Ni ₄ Dy ₂ W ₂]. 10(CH ₃ CN).2H ₂ O	[C ₁₀₀ H ₁₀₀ N ₂₄ O ₁₈ Ni ₄ Y ₂ W ₂]. 10(CH ₃ CN).2H ₂ O	[C ₉₆ H ₉₆ Co ₂ N ₁₈ Ni ₄ O ₂₀ Tb ₂]. 2(C ₃ H ₆ O).2H ₂ O
Asymmetric unit contain	C ₁₂₀ H ₁₃₄ N ₃₄ Ni ₄ O ₂₀ Tb ₂ W ₂	C ₁₂₀ H ₁₃₄ N ₃₄ Ni ₄ O ₂₀ Dy ₂ W ₂	C ₁₂₀ H ₁₃₄ N ₃₄ Ni ₄ O ₂₀ Y ₂ W ₂	C ₅₁ H ₅₄ CoN ₅ Ni ₂ O ₁₆ Tb
Formula weight	3292.98	3300.14	3152.96	2640.54
Temperature	150(2) K	150(2) K	150(2) K	180(2) K
Wavelength	0.71073 Å	0.71073 Å	0.71073 Å	0.71073 Å
Crystal system	Triclinic	Triclinic	Triclinic	Monoclinic
Space group	P -1	P -1	P -1	P 1 21/c 1
Unit cell dimensions	a = 16.7341(8) Å b = 20.6199(8) Å c = 20.8979(8) Å α= 87.881(5)° β= 89.214(5)°. γ = 74.309(5)°	a = 16.7120(10) Å b = 20.624(2) Å c = 20.852(3) Å α= 87.814(2)° β= 89.178(3)° γ = 74.215(2)°	a = 16.710(1) Å b = 20.663(1) Å c = 20.852(1) Å α= 87.797(1)°. β= 89.185(1)°. γ = 74.158(1)°.	a = 16.8968(7) Å b = 22.2820(7) Å c = 19.3332(8) Å α= 90 °. β= 106.728 (4)°. γ = 90 °.
Volume	6937.4(5) Å ³	6910.9(13) Å ³	6921.1(6) Å ³	6970.8(5) Å ³
Z	2	2	2	2
Density (calculated)	1.576 Mg/m ³	1.586 Mg/m ³	1.513 Mg/m ³	1.256 Mg/m ³
Absorption coefficient	3.259 mm ⁻¹	3.330 mm ⁻¹	3.088 mm ⁻¹	1.820 mm ⁻¹
F(000)	3284	3288	3180	2664
Crystal size	0.200 x 0.150 x 0.150 mm ³	0.200 x 0.150 x 0.150 mm ³	0.160 x 0.120 x 0.120 mm ³	0.18 x 0.1 x 0.02 mm ³
Theta range for data collection	3.417 to 26.373°.	3.417 to 26.372°.	3.411 to 26.372°.	3.37 to 25.68°
Index ranges	-20<=h<=20, -24<=k<=25, -26<=l<=26	-20<=h<=20, -25<=k<=25, -26<=l<=26	-20<=h<=20, -25<=k<=25, -26<=l<=26	-20<=h<=20, -26<=k<=27, -23<=l<=23
Reflections collected	51437	55836	55372	54665
Independent reflections	28124 [R(int) = 0.0904]	28139 [R(int) = 0.0552]	28125 [R(int) = 0.0324]	13197 [R(int) = 0.0745]
Completeness to theta = 25.242°	99.1 %	99.6 %	99.4 %	25.68 99.7 %
Absorption correction	Empirical	Empirical	Empirical	Semi-empirical from equivalents
Max. and min. transmission	0.6406 and 0.5618	0.6350 and 0.5556	0.7082 and 0.6379	0.978 and 0.811
Refinement method	Full-matrix least-squares on F ²	Full-matrix least-squares on F ²	Full-matrix least-squares on F ²	Full-matrix least-squares on F ²
Data / restraints / parameters	28124 / 0 / 1633	28139 / 0 / 1637	28125 / 0 / 1665	13197 / 0 / 695
Goodness-of-fit on F ²	1.114	1.164	1.115	0.890
Final R indices [I>2sigma(I)]	R1 = 0.0976, wR2 = 0.2174	R1 = 0.0637, wR2 = 0.1374	R1 = 0.0379, wR2 = 0.0758	R1 = 0.0673, wR2 = 0.1599
R indices (all data)	R1 = 0.1262, wR2 = 0.2307	R1 = 0.0932, wR2 = 0.1463	R1 = 0.0541, wR2 = 0.0800	R1 = 0.1038, wR2 = 0.1687
Largest diff. peak and hole	5.561 and -1.379 e.Å ⁻³	3.105 and -1.463 e.Å ⁻³	1.894 and -0.918 e.Å ⁻³	11.322 and -1.055 e.Å ⁻³

Figure S1. [$\{L^{Me_2}NiTb(H_2O)NiL^{Me_2}\}W(CN)_8]_2 \cdot 10MeCN \cdot 2H_2O$, **1a**: views of (*top*) the asymmetric unit (ellipsoid plot with 30 % occupancy level) and (*bottom*) the molecular fragments with atom labels (H atoms and solvents molecules are not shown for clarity), and selected distances and angles.



Selected bond lengths (Å)

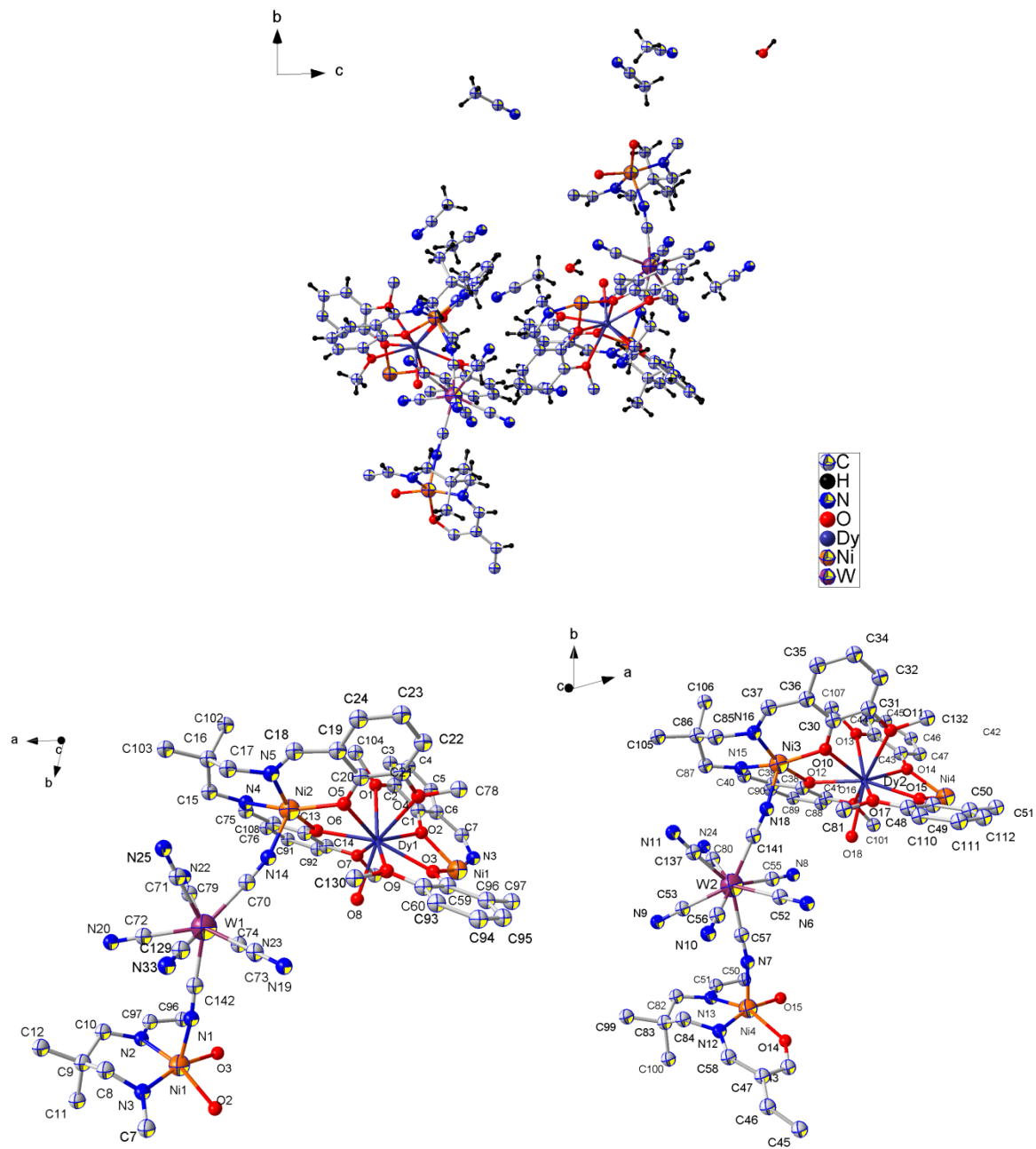
Ni1	N1	1.9789(130)	W2	C53	2.1613(176)	N16	C85	1.4775(193)
Ni1	N3	1.9933(116)	W2	C80	2.1643(151)	N18	C141	1.2169(228)
Ni1	O2	2.0044(82)	W2	C56	2.1724(150)	N19	C73	1.1720(195)
Ni1	O3	2.0071(93)	W2	C55	2.1770(147)	N20	C72	1.1817(204)
Ni1	N2	2.0181(111)	Tb1	O8	2.3090(128)	N22	C79	1.1429(202)
Ni2	N14	1.9867(133)	Tb1	O5	2.3349(95)	N23	C74	1.1377(185)
Ni2	O6	1.9931(86)	Tb1	O2	2.3352(98)	N24	C80	1.1416(215)
Ni2	N4	2.0150(113)	Tb1	O3	2.3836(90)	N25	C71	1.1395(168)
Ni2	N5	2.0173(119)	Tb1	O6	2.3914(98)	N26	C113	1.1194(287)
Ni2	O5	2.0429(107)	Tb1	O1	2.4935(102)	N27	C123	1.1299(407)
Ni3	O12	1.9910(87)	Tb1	O4	2.5197(110)	N28	C125	1.1324(311)
Ni3	N16	1.9935(123)	Tb1	O9	2.5757(104)	N29	C127	1.0976(315)
Ni3	N18	2.0084(133)	Tb1	O7	2.5794(87)	N30	C115	1.1026(305)
Ni3	N15	2.0096(119)	Tb2	O18	2.2897(133)	N31	C121	1.1153(263)
Ni3	O10	2.0121(105)	Tb2	O10	2.3325(87)	N32	C117	1.1203(418)
Ni4	N7	1.9814(131)	Tb2	O15	2.3658(89)	N33	C129	1.1258(212)
Ni4	O14	1.9949(88)	Tb2	O14	2.3692(95)	N34	C119	1.1264(329)
Ni4	N13	2.0067(114)	Tb2	O12	2.4037(97)	N35	C135	1.1308(324)
Ni4	N12	2.0145(111)	Tb2	O13	2.5005(100)	N38	C139	1.0760(396)
Ni4	O15	2.0214(89)	Tb2	O11	2.5206(109)	N1	C142	1.2298(206)
W1	C142	2.0726(168)	Tb2	O16	2.5694(108)	N2	C97	1.2953(178)
W1	C72	2.1397(145)	Tb2	O17	2.5763(102)	N2	C10	1.4841(191)
W1	C73	2.1406(152)	N10	C56	1.1502(209)	N3	C7	1.2916(167)
W1	C79	2.1713(146)	N11	C137	1.1605(185)	N3	C8	1.4539(179)
W1	C71	2.1722(125)	N12	C58	1.2682(176)	N4	C75	1.2980(197)
W1	C70	2.1739(165)	N12	C84	1.4508(172)	N4	C15	1.4678(188)
W1	C74	2.1773(139)	N13	C51	1.3144(207)	N5	C18	1.2818(204)
W1	C129	2.1801(149)	N13	C82	1.4765(182)	N5	C17	1.4762(182)
W2	C141	2.0665(179)	N14	C70	1.1461(213)	N6	C52	1.1547(187)
W2	C57	2.1332(146)	N15	C40	1.2683(195)	N7	C57	1.1840(192)
W2	C137	2.1585(143)	N15	C87	1.4937(189)	N8	C55	1.1574(197)
W2	C52	2.1603(151)	N16	C37	1.2751(211)	N9	C53	1.1694(230)

Angles (°)

Ni1-N1-W1, 163.8(5); Ni2-N14-W1, 158.7(5); Ni3-N18-W2, 152.5(5); Ni4-N7-W2, 169.3(5);

Angles between planes: [Ni1-O2-O2] / [Ni2-O5-O6], 62.7(5)°; [Ni3-O10-O12] / [Ni4-O14-O15], 62.3(3)°.

Figure S2. $[\{L^{Me_2}NiDy(H_2O)NiL^{Me_2}\}W(CN)_8]_2 \cdot 10MeCN \cdot 2H_2O$, **2a:** views of (*top*) the asymmetric unit (ellipsoid plot with 30 % occupancy level) and (*bottom*) the molecular fragments with atom labels (H atoms and solvents molecules are not shown for clarity), and selected distances and angles.



Selected bond lengths (Å):

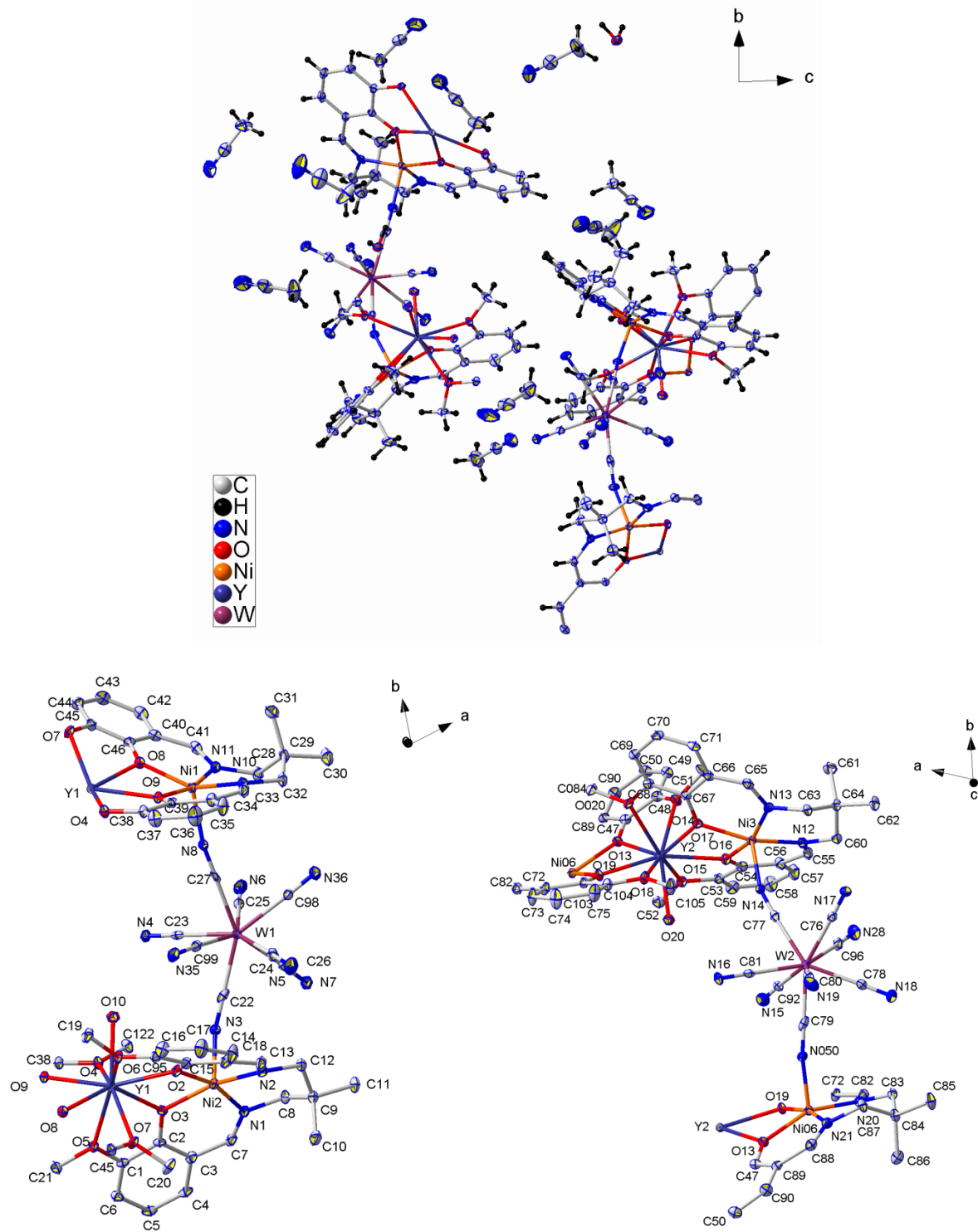
Dy1	O8	2.3012(85)	W2	C52	2.1660(93)	N16	C85	1.4644(144)
Dy1	O5	2.3237(59)	W2	C55	2.1701(108)	N18	C141	1.1711(147)
Dy1	O2	2.3339(69)	Ni1	N1	1.9926(87)	N19	C73	1.1550(141)
Dy1	O3	2.3555(60)	Ni1	O2	1.9968(57)	N20	C72	1.1620(164)
Dy1	O6	2.3775(65)	Ni1	N2	1.9995(79)	N22	C79	1.1393(142)
Dy1	O1	2.4995(61)	Ni1	N3	1.9996(88)	N23	C74	1.1421(132)
Dy1	O4	2.5044(68)	Ni1	O3	2.0053(67)	N24	C80	1.1323(145)
Dy1	O7	2.5771(63)	Ni2	N14	1.9794(90)	N25	C71	1.1368(122)
Dy1	O9	2.5792(66)	Ni2	O6	1.9940(62)	N26	C113	1.1326(200)
Dy2	O18	2.3047(90)	Ni2	N4	2.0127(82)	N27	C123	1.134(30)
Dy2	O10	2.3254(59)	Ni2	N5	2.0187(80)	N28	C125	1.1149(234)
Dy2	O14	2.3558(66)	Ni2	O5	2.0352(71)	N29	C127	1.1400(245)
Dy2	O15	2.3580(59)	Ni3	O12	1.9856(62)	N30	C115	1.1414(221)
Dy2	O12	2.3788(65)	Ni3	N18	1.9959(88)	N31	C121	1.1281(194)
Dy2	O13	2.497(6)	Ni3	N15	2.0028(83)	N32	C117	1.1087(285)
Dy2	O11	2.5151(71)	Ni3	N16	2.0059(82)	N33	C129	1.1536(153)
Dy2	O16	2.5626(66)	Ni3	O10	2.0249(70)	N34	C119	1.1420(227)
Dy2	O17	2.5666(61)	Ni4	O14	1.9949(56)	N35	C135	1.1492(215)
W1	C142	2.0868(104)	Ni4	N7	1.9967(88)	N38	C139	1.0990(262)
W1	C72	2.1375(123)	Ni4	N13	2.0027(80)	N1	C142	1.1978(132)
W1	C73	2.1517(108)	Ni4	O15	2.0083(65)	N2	C97	1.2961(134)
W1	C129	2.1621(109)	Ni4	N12	2.0158(85)	N2	C10	1.4811(136)
W1	C70	2.1632(122)	N10	C56	1.1587(150)	N3	C7	1.2945(125)
W1	C79	2.1672(101)	N11	C137	1.1693(136)	N3	C8	1.4603(119)
W1	C71	2.1747(95)	N12	C58	1.2856(129)	N4	C75	1.2819(150)
W1	C74	2.1765(103)	N12	C84	1.4637(119)	N4	C15	1.4864(128)
W2	C57	2.1033(124)	N13	C51	1.2982(132)	N5	C18	1.2919(147)
W2	C141	2.1109(114)	N13	C82	1.4936(125)	N5	C17	1.4781(132)
W2	C137	2.1545(95)	N14	C70	1.1635(152)	N6	C52	1.1445(121)
W2	C56	2.1586(108)	N15	C40	1.2747(136)	N7	C57	1.1949(149)
W2	C80	2.1620(103)	N15	C87	1.5120(127)	N8	C55	1.1471(150)
W2	C53	2.1638(108)	N16	C37	1.2912(152)	N9	C53	1.1502(154)

Selected angles (°):

Ni1-N1-W1, 164.0(4); Ni2-N14-W1, 158.6(4); Ni3-N18-W2, 153.0(4); Ni4-N7-W2, 169.6(4).

Angles between planes: [O2-Ni1-O3]/[O5-Ni2-O6], 63.4(2)°; [O10-Ni3-O12]/[O14-Ni4-O15], 63.3(2)°.

Figure S3. $[\{L^{Me_2}NiY(H_2O)NiL^{Me_2}\}W(CN)_8]_2 \cdot 10MeCN \cdot 2H_2O$, **1c**: ORTEP plots of (*top*) the asymmetric unit (ellipsoid plot with 30 % occupancy level) and (*bottom*) the molecular fragments with atom labels (H atoms and solvents molecules are not shown for clarity), and selected distances and angles.



Selected bond lengths (Å):

Y1	O3	2.3080(27)	W2	C76	2.1694(38)	C98	N36	1.1491(74)
Y1	O10	2.3091(34)	W2	C92	2.1700(42)	C99	N35	1.1571(63)
Y1	O8	2.3396(29)	C7	N1	1.2853(64)	C100	N22	1.1372(91)
Y1	O9	2.3480(25)	C8	N1	1.4772(60)	C110	N23	1.141(10)
Y1	O2	2.3740(28)	C12	N2	1.4769(57)	C120	N24	1.1411(89)
Y1	O7	2.4822(28)	C13	N2	1.2746(58)	C130	N25	1.1253(107)
Y1	O5	2.5049(34)	C22	N3	1.1659(64)	C140	N27	1.1330(106)
Y1	O6	2.5467(31)	C23	N4	1.1541(55)	C150	N26	1.1289(82)
Y1	O4	2.5643(29)	C24	N5	1.1311(56)	C160	N30	1.1241(132)
Y2	O17	2.3083(27)	C25	N6	1.1551(59)	C180	N31	1.1256(115)
Y2	O20	2.3126(33)	C26	N7	1.1455(55)	C190	N33	1.1110(117)
Y2	O13	2.3151(30)	C27	N8	1.1719(58)	C200	N34	1.1296(106)
Y2	O19	2.3526(26)	C28	N11	1.4649(53)	Ni1	O8	1.9928(25)
Y2	O16	2.3724(30)	C32	N10	1.4867(56)	Ni1	N8	1.9936(41)
Y2	O020	2.4890(33)	C33	N10	1.2902(55)	Ni1	N10	2.0032(33)
Y2	O14	2.4899(29)	C41	N11	1.2837(52)	Ni1	O9	2.0075(28)
Y2	O18	2.5725(30)	C55	N12	1.2819(56)	Ni1	N11	2.0196(38)
Y2	O15	2.5789(30)	C60	N12	1.4769(58)	Ni2	O2	1.9881(28)
W1	C22	2.1264(50)	C63	N13	1.4716(60)	Ni2	N3	1.9903(39)
W1	C27	2.1288(42)	C65	N13	1.2801(62)	Ni2	N1	2.0032(37)
W1	C25	2.1629(42)	C76	N17	1.1498(52)	Ni2	N2	2.0138(35)
W1	C23	2.1636(45)	C77	N14	1.1552(63)	Ni2	O3	2.0314(32)
W1	C98	2.1653(53)	C78	N18	1.1552(74)	Ni3	N14	1.9899(38)
W1	C26	2.1692(40)	C79	N050	1.1761(72)	Ni3	O16	1.9968(29)
W1	C99	2.1701(44)	C80	N19	1.1424(61)	Ni3	N13	2.0148(36)
W1	C24	2.1717(40)	C81	N16	1.1481(56)	Ni3	N12	2.0178(34)
W2	C79	2.1106(62)	C82	N20	1.2965(56)	Ni3	O17	2.0421(30)
W2	C78	2.1479(52)	C83	N20	1.4840(57)	Ni06	N050	1.9895(39)
W2	C81	2.1601(46)	C87	N21	1.4708(52)	Ni06	O13	2.0010(25)
W2	C80	2.1620(43)	C88	N21	1.2911(52)	Ni06	N21	2.0013(38)
W2	C77	2.1658(51)	C92	N15	1.1507(58)	Ni06	O19	2.0017(29)
W2	C96	2.1686(41)	C96	N28	1.1417(58)	Ni06	N20	2.0051(32)

Selected angles (°):

Ni1-N8-W1, 169.9(1); Ni2-N3-W1, 153.7(2), Ni3-N14-W2, 158.4(1); Ni6-N50-W2, 163.7(2)°.

Between planes: [O8-Ni1-O9]/[O2-Ni2-O3], 63.0(1); [O16-Ni3-O17]/[O13-Ni6-O19], 63.3(1)°.

Figure S4. $\left[\{L^{Me^2}NiTb(H_2O)NiL^{Me^2}\}Co(CN)_6\right]_2 \cdot 2Me_2CO \cdot 2H_2O$, **2**: ORTEP (ellipsoid plot with 30 % occupancy level).

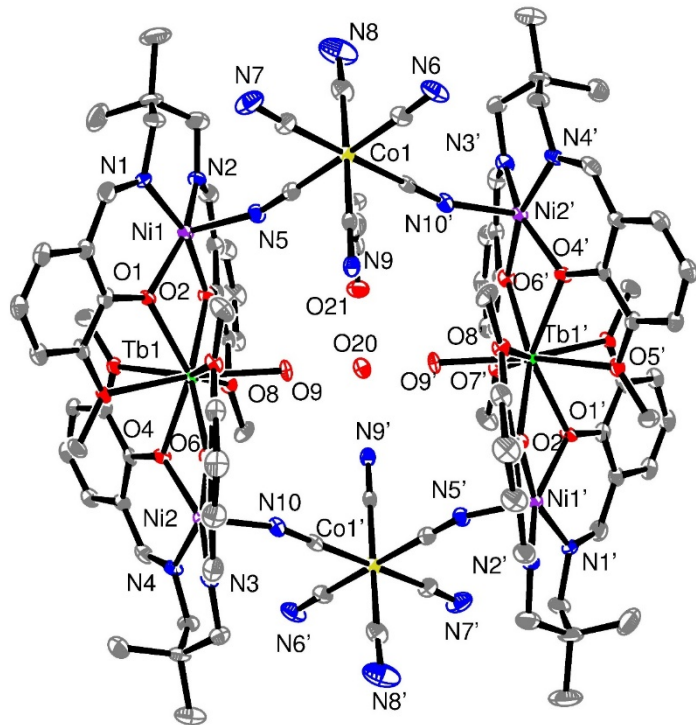


Table S2: Continuous Shape Measures calculations for the nona-coordinated Ln centres in **1a-c** and **2**.¹⁰

S H A P E v2.1 Continuous Shape Measures calculation
 (c) 2013 Electronic Structure Group, Universitat de Barcelona

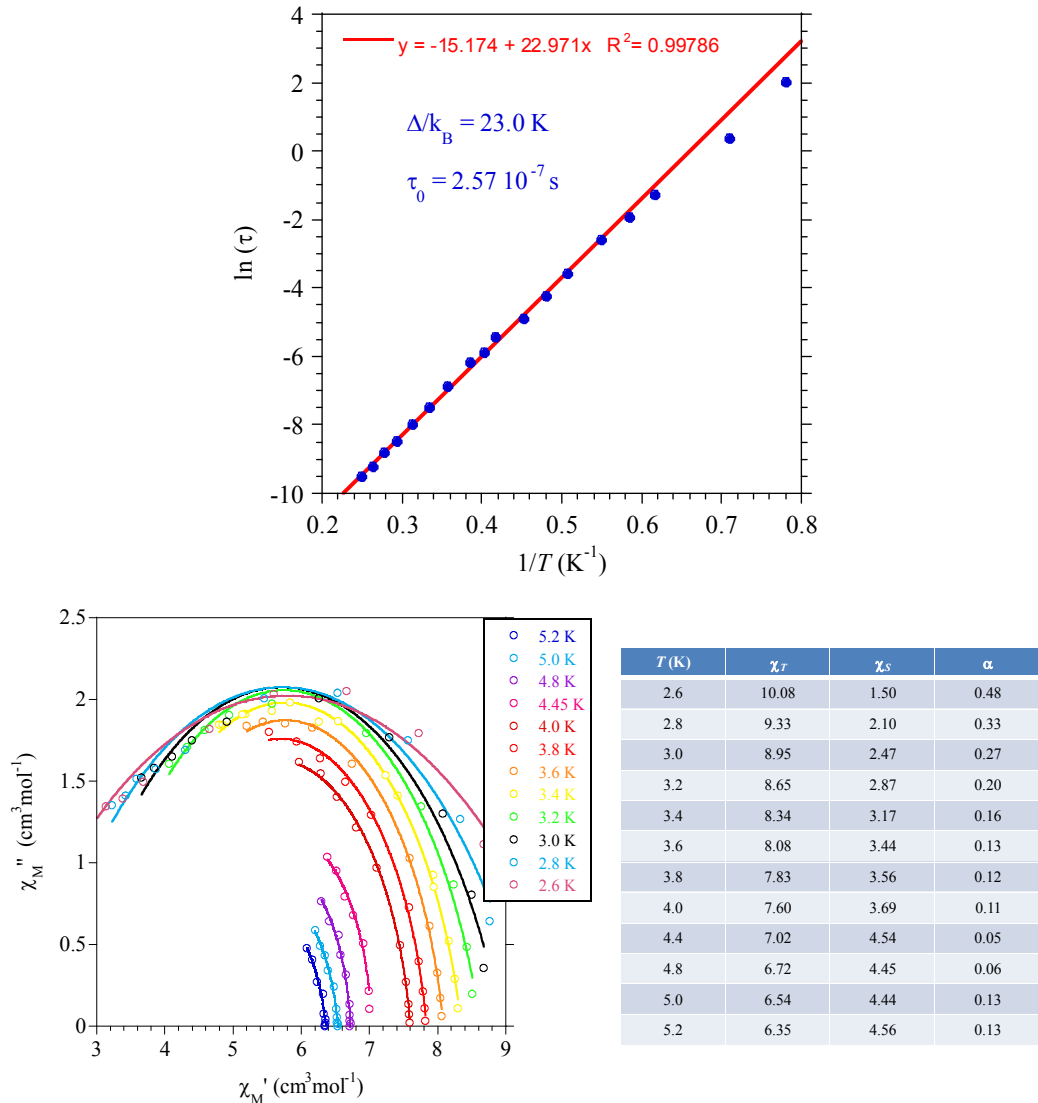
CSAPR-9 (C_{4v}) Spherical capped square antiprism
 JTCTPR-9 (D_{3h}) Tricapped trigonal prism J51
 JTDIC-9 (C_{3v}) Tridiminished icosahedron J63

[ML ₉]	CSAPR-9	JTCTPR-9	JTDIC-9
Tb1 (1a)	4.1190	2.8060	2.9480
Tb2 (1a)	3.8880	2.6100	3.0450
Dy1 (1b)	4.0170	2.7120	2.8620
Dy2 (1b)	3.7830	2.4860	2.9070
Y1 (1c)	3.7420	2.4450	2.8960
Y2 (1c)	4.0190	2.6820	2.7990
Tb (2)	3.9780	2.6220	2.6410

¹⁰ M. Llunell, D. Casanova, J. Cirera, P. Alemany and S. Alvarez, *SHAPE: Program for the stereochemical analysis of molecular fragments by means of continuous shape measures and associated tools*, (2013) University of Barcelona, Barcelona. A. Ruiz-Martínez, D. Casanova and S. Alvarez, *Chem. Eur. J.*, 2008, **14**, 1291.

Figure S5. AC susceptibility data for **1a** and **1b**:

1a: (top) Experimental $\ln\tau = f(T^{-1})$ with best fit parameters, (bottom) Cole-Cole plots with best-fits (solid lines) of a generalized Debye model, and detail of the fitting parameters where χ_T stands for the isothermal susceptibility, χ_S the adiabatic susceptibility, and α accounts for the width of the τ distribution.



1b: (top) Experimental $\ln\tau = f(T^{-1})$ with best fit parameters, (bottom) Cole-Cole plots with best-fits (solid lines) of a generalized Debye model, and detail of the fitting parameters where χ_T stands for the isothermal susceptibility, χ_s the adiabatic susceptibility, and α accounts for the width of the τ distribution.

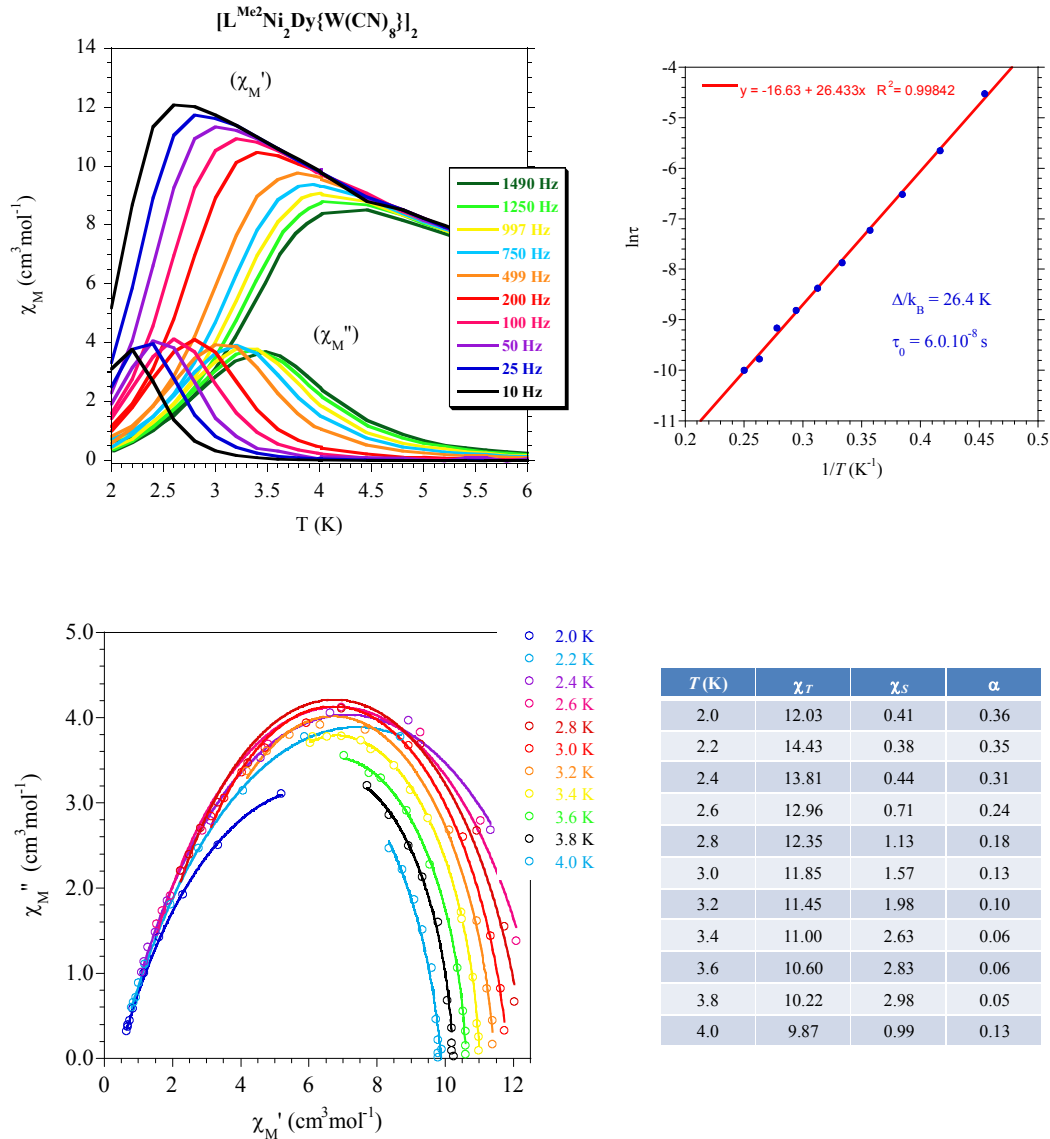


Figure S6. Magnetic behaviors for $\left[\{L^{Me^2}NiTb(H_2O)NiL^{Me^2}\}Co(CN)_6\right]_2$, **2**: (top) temperature dependence of the magnetic susceptibility plotted as cMT, and field dependence of the magnetization recorded for 2 K; (bottom) AC susceptibility recorded for two frequencies (100 and 997 Hz) with $H_{DC} = 0$ and 1 kOe.

